J|A|C|S
ARTICLES
Published on Web 03/20/2004

Tetraorganylammonium Superoxide Compounds: Close to Unperturbed Superoxide Ions in the Solid State

Pascal D. C. Dietzel, Reinhard K. Kremer, and Martin Jansen*

Contribution from the Max-Planck-Institut für Festkörperforschung, Heisenbergstrasse 1, D-70689 Stuttgart, Germany

Received December 1, 2003; E-mail: m.jansen@fkf.mpg.de

Abstract: Trimethylphenylammonium superoxide (**1**) and tetrabutylammonium superoxide (**2**) were prepared by ion-exchange reaction in liquid ammonia. Both compounds were structurally characterized by single-crystal X-ray diffraction. The crystal structure of **2** contains solvent ammonia molecules that are hydrogen bonded to the superoxide ion and therefore may influence the bonding properties of the superoxide ion. The crystal structure of **1** does not contain any solvent molecules. Therefore, it represents the best known approximation to the virtually isolated superoxide ion in the solid state to date. The O−O bond length is 1.332(2) Å in **1** and 1.312(2) Å in **2**. Magnetization measurements show that the susceptibilities of both compounds follow an ideal Curie law down to 2 K reflecting an absence of intermolecular exchange effects between the superoxide ions. The effective magnetic moments of both compounds are larger than the spin-only value due to contributions of the orbital momentum in the superoxide ion. The values of the magnetic moment comply well with the *g* factors obtained from electron paramagnetic resonance spectra. The *g* tensors themselves reflect the anisotropic environment of the superoxide ions. The Π_g energy levels which are degenerate in the free superoxide ion split up in crystal fields of lower than tetragonal symmetry. The energy splitting is estimated from the diagonal elements of the *g* tensor of **1**.

Introduction

Complexes of dioxygen coordinating to a metal center play a significant role in biological processes, and their study lies at the core of bioinorganic chemistry. Such metal−dioxygen complexes are usually classified as superoxo and peroxo complexes, depending on the O−O bond length and the O−O stretching frequency.[1] Numerous superoxo complexes have been characterized.[2,3] They formally contain the superoxide group O_2^-. Because the electronic structure of the superoxide moiety is influenced by bonding to the metal atoms, the O−O bond length varies in this class of compounds.[3] The 17 electron superoxide ion is one of the few isolable paramagnetic main group ions, and it represents one of the intermediate species in most reduction reactions of molecular oxygen. This fact in itself should be sufficient to warrant an interest in the chemistry of the superoxide ion. It comes as a surprise, though, to realize that knowledge of the free, uninfluenced by bonding to another chemical entity, superoxide group is rather limited. This is partly due to the paucity of pure superoxide compounds that can be obtained in the bulk. Thoroughly investigated among these are the alkali metal superoxides.[4−38] The compounds of the heavier alkali metals potassium, rubidium, and cesium are the thermodynamic stable products of the reaction of the corresponding metal with oxygen at ambient pressure. They would therefore appear to be suitable and easily accessible systems for the study of the superoxide ion in the solid state. Unfortunately, the superoxide ions interact significantly in the alkali metal superoxides, which leads to exchange effects that influence for instance their magnetic properties. Concurrently, adjustments in the orientation of the superoxide ions in the crystal structure lead to miscellaneous phase transitions that complicate structural investigations. In addition, the superoxide ion is prone to rotational disorder at sufficiently high temperatures. Consequently, the O−O distance of the superoxide in the solid state could only be determined imprecisely until now.

(1) Vaska, L. *Acc. Chem. Res.* **1976**, *9*, 175−183.
(2) (a) Gubelmann, M. H.; Williams, A. F. *Struct. Bonding* **1983**, *55*, 2−65. (b) Martell, A. E., Sawyer, D. T., Eds. *Oxygen Complexes and Oxygen Activation by Transition Metal Complexes*; Plenum Press: New York, 1988. (c) Klotz, I. M.; Kurtz, D. M. *Chem. Rev.* **1994**, *94*, 567−568.
(3) Cramer, C. J.; Tolman, W. B.; Theopold, K. H.; Rheingold, A. L. *Proc. Natl. Acad. Sci. U.S.A.* **2003**, *100*, 3635−3640.
(4) Kassatochkin, W.; Kotow, W. *J. Chem. Phys.* **1936**, *4*, 458.
(5) Stephanou, S. E.; Schechter, W. H.; Argersinger, W. J., Jr.; Kleinberg, J. *J. Am. Chem. Soc.* **1949**, *71*, 1819−1821.
(6) Schechter, W. H.; Thompson, J. K.; Kleinberg, J. *J. Am. Chem. Soc.* **1949**, *71*, 1816−1818.
(7) Templeton, D. H.; Dauben, C. H. *J. Am. Chem. Soc.* **1950**, *72*, 2251−2254.
(8) Seyb, E.; Kleinberg, J. *J. Am. Chem. Soc.* **1951**, *73*, 2308−2309.
(9) Zhdanov, G. S.; Zvonkova, Z. V. *Dokl. Akad. Nauk SSSR* **1952**, *82*, 743−746.
(10) Carter, G. F.; Templeton, D. H. *J. Am. Chem. Soc.* **1953**, *75*, 5247−5249.
(11) Abrahams, S. C.; Kalnajs, J. *Acta Crystallogr.* **1955**, *8*, 503−506.
(12) Bennett, J. E.; Ingram, D. J. E.; Symons, M. C. R.; George, P.; Griffith, J. S. *Philos. Mag.* **1955**, *46*, 443−444.
(13) Brame, E. G.; Cohen, S.; Margrave, J. L.; Meloche, V. W. *J. Inorg. Nucl. Chem.* **1957**, *4*, 90−92.
(14) McLachlan, A. D.; Symons, M. C. R.; Townsend, M. G. *J. Chem. Soc.* **1959**, 952−957.
(15) Halverson, F. *J. Phys. Chem. Solids* **1962**, *23*, 207−214.
(16) Creighton, J. A.; Lippincott, E. R. *J. Chem. Phys.* **1964**, *40*, 1779−1780.
(17) Sparks, J. T.; Komoto, T. *J. Appl. Phys.* **1966**, *37*, 1040−1041.
(18) Smith, H. G.; Nicklow, R. M.; Raubenheimer, L. J.; Wilkinson, M. K. *J. Appl. Phys.* **1966**, *37*, 1047−1049.

In an attempt to study the properties of the isolated, quasi-free superoxide ion, we decided to synthesize ionic superoxides of bulky and anisotropic cations. Through this approach, we were intending to keep the anions at a far enough distance from each other to widely suppress intermolecular interactions and to lock the O_2^- moiety in a fixed orientation. These cations need to be stable against the superoxide ion and should allow for a synthesis of superoxide compounds in a suitable solvent. Tetraorganylammonium ions appear to fulfill these prerequisites: they are known to behave chemically similar to the alkali metal cations and form isolable superoxide compounds,[39−41] they are larger than the alkali metal cations, and their shape can be taylored through variation of the substituents. Liquid ammonia is a suitable solvent, in which the superoxide ion is stable, and cation exchange has been shown to be an efficient approach to synthesize novel compounds in this solvent. This technique was originally developed for the synthesis of ionic ozonides,[42] but has recently been shown to work with superoxides[41] and even with the auride ion, too.[43] Here, we report the synthesis and structural and physical characterization of trimethylphenylammonium superoxide **1** and tetrabutylammonium superoxide **2**.

Experimental Section

General. (**Caution!** Superoxide salts with organic cations are potentially explosive and should be handled with care and in small amounts only.) All operations have been carried out under inert conditions either in a vacuum or in a dry argon atmosphere using standard Schlenk techniques. Ammonia (grade 3.8, Messer-Griesheim) was liquified and stored over potassium metal at −78 °C.

Starting Materials. Potassium superoxide was prepared by oxidation of potassium metal with oxygen. Tetramethylammonium hydroxide pentahydrate (99%, Acros) was dried to the monohydrate and converted into tetramethylammonium superoxide by metathesis reaction with potassium superoxide according to procedures described elsewhere.[40]

Trimethylphenylammonium iodide (99%, Avocado) and tetrabutylammonium bromide (99%+, Fluka) were each dissolved in methanol (HPLC grade, Riedel-de-Haën) and converted into the corresponding hydroxide by vigorous stirring with freshly precipitated silver oxide for 2 h and subsequent filtration. A 0.9 molar amount (referring to active sites) of the acidic form of the ion-exchange resin (type Amberlyst 15, Merck) was then added to the solutions. After 5 days, the ion-exchange resin was separated from the solution by filtration, washed several times with methanol, and thoroughly dried at 105 °C in a dynamic vacuum.

$[N(CH_3)_3(C_6H_5)](O_2)$ (1). First, 1.5 g of ion-exchange resin was put into a leg of an H-shaped glass apparatus whose two sides are connected via a glass filter sieve of porosity 3. At −78 °C, 106 mg (1 mmol) of tetramethylammonium superoxide was added to the ion-exchange resin. Next, ∼25 mL of ammonia was condensed into the reaction vessel. The solution was warmed once to −35 °C to dissolve the tetramethylammonium superoxide and allowed to react for 24 h at −50 °C, after which it was separated from the ion-exchange resin by filtration into the other leg of the apparatus. Slow evaporation of the ammonia yielded pale yellow crystals.

$[N(C_4H_9)_4](O_2)$ (2). Synthesis is analogous to that of **1**. However, to obtain crystals suitable for single-crystal X-ray analysis, the evaporation of the ammonia has to be stopped when a crop of crystals has formed in the concentrated solution. We will further denote the compound isolated from this solution as **2a**. Complete removal of ammonia yielded the ammonia-free amorphous compound **2b** that was used in the physical measurements.

X-ray Crystallography. Crystals of **1** (cuboid, pale yellow) were selected under a microscope from an inert oil (perfluorinated polyether, Riedel de Haën) cooled in a stream of nitrogen gas to −50 °C.[44] They were picked up with a nylon loop attached to the goniometer head (Hamilton Research), transferred in liquid nitrogen, and mounted onto the diffractometer in a cooling stream. Intensities of Bragg reflections were measured at −150 °C with a Stoe Stadi4 four-circle diffractometer using Mo Kα radiation.

Crystals of **2a** (block, pale yellow) were selected in an analogous procedure with the difference that they were transferred into the cooled perfluorinated polyether in their mother liquor. Data were collected with a Stoe-IPDS area detector diffractometer at −180 °C using Ag Kα radiation.

Structure solution and parameter refinement was performed using the SHELX97 software suite.[45] Parameters were refined using full-matrix least squares against F^2. All non-hydrogen atomic parameters were refined allowing for anisotropic displacement. Hydrogen atoms were located in the difference electron density maps. For **1**, the hydrogen atoms were refined using a common isotropic displacement parameter. Restraints were applied to bond lengths for chemically similar C−H bonds. **1** crystallizes in an acentric space group. Because there are no heavier atoms than oxygen present in the structure, it was not possible to determine the absolute structure. Therefore, Friedel pairs were merged before final refinement. For **2a**, restraints were applied to the N−H bond lengths in the ammonia molecules. Details of the data collections and structure refinements are listed in Table 1.

Physical Measurements. Raman spectra at room temperature in the range from 200 to 3500 cm^{-1} were recorded with a Jobin Yvon Horiba laser Raman microscope spectrometer type Labram employing a He−

(19) (a) Blunt, F. J.; Hendra, P. J.; Mackenzie, J. R. *J. Chem. Soc., Chem. Commun.* **1969**, 278−279. (b) Bates, J. B.; Brooker, M. H.; Boyd, G. E. *Chem. Phys. Lett.* **1972**, *16*, 391−395.
(20) (a) Bösch, M.; Känzig, W. *Helv. Phys. Acta* **1973**, *46*, 17. (b) Bösch, M.; Känzig, W. *Phys. Condens. Matter* **1973**, *16*, 107−112.
(21) Dudarev, V. Y.; Tsentsiper, A. B.; Dobrolyubova, M. S. *Sov. Phys. Crystallogr.* **1974**, *18*, 477−479.
(22) Zumsteg, A.; Ziegler, M.; Känzig, W.; Bösch, M. *Phys. Condens. Matter* **1974**, *17*, 267−291.
(23) Bösch, M.; Känzig, W. *Helv. Phys. Acta* **1975**, *48*, 743−785.
(24) Khan, A. U.; Mahanti, S. D. *J. Chem. Phys.* **1975**, *63*, 2271−2278.
(25) Ziegler, M.; Meister, H. R.; Känzig, W. *Helv. Phys. Acta* **1975**, *48*, 599−607.
(26) Mahanti, S. D.; Khan, A. U. *Solid State Commun.* **1976**, *18*, 159−162.
(27) Ziegler, M.; Rosenfeld, M.; Känzig, W.; Fischer, P. *Helv. Phys. Acta* **1976**, *49*, 57−90.
(28) Rosenfeld, M.; Ziegler, M.; Känzig, W. *Helv. Phys. Acta* **1978**, *51*, 298−320.
(29) (a) Kemeny, G.; Mahanti, S. D. *Phys. Rev. B* **1979**, *20*, 2961−2963. (b) Mahanti, S. D.; Kemeny, G. *Phys. Rev. B* **1979**, *20*, 2105−2117.
(30) Labhart, M.; Raoux, D.; Känzig, W. *Helv. Phys. Acta* **1977**, *50*, 602−603.
(31) Labhart, M.; Raoux, D.; Känzig, W.; Bösch, M. A. *Phys. Rev. B* **1979**, *20*, 53−70.
(32) Bösch, M. A.; Lines, M. E.; Labhart, M. *Phys. Rev. Lett.* **1980**, *45*, 140−143.
(33) Kemeny, G.; Kaplan, T. A.; Mahanti, S. D.; Sahu, D. *Phys. Rev. B* **1981**, *24*, 5222−5228.
(34) (a) Lines, M. E.; Bösch, M. A. *Phys. Rev. B* **1981**, *23*, 263−270. (b) Lines, M. E. *Phys. Rev. B* **1981**, *24*, 5248−5259.
(35) Biljana, S. *Thermochim. Acta* **1985**, *92*, 231−234.
(36) (a) Bertel, E.; Netzer, F. P.; Rosina, G.; Saalfeld, H. *Phys. Rev. B* **1989**, *39*, 6082−6086. (b) Pedio, M.; Benfatto, M.; Aminpirooz, S.; Haase, J. *Europhys. Lett.* **1993**, *21*, 239−244.
(37) Kadam, R. M.; Sastry, M. D. *Phase Transitions A* **1997**, *60*, 79−87.
(38) Krawietz, T. R.; Murray, D. K.; Haw, J. F. *J. Phys. Chem. A* **1998**, *102*, 8779−8785.
(39) (a) McElroy, A. D.; Hashman, J, S. *Inorg. Chem.* **1964**, *3*, 1798−1799. (b) Latysheva, E. I.; Cherkasov, E. N.; Tokareva, S. A.; Velikova, N. G.; Vol'nov, I. I. *Bull. Acad. Sci. SSR Chimija* **1974**, *23*, 1610−1612.
(40) (a) Sawyer, D. T.; Calderwood, T. S.; Yamaguchi, K.; Angelis, C. T. *Inorg. Chem.* **1983**, *22*, 2577−2583. (b) Yamaguchi, K.; Calderwood, T. S.; Sawyer, D. T. *Inorg. Chem.* **1986**, *25*, 1289−1290.
(41) Seyeda, H.; Jansen, M. *J. Chem. Soc., Dalton Trans.* **1998**, *6*, 875−876.
(42) (a) Korber, N.; Jansen, M. *Chem. Ber.* **1992**, *125*, 1383−1388. (b) Korber, N.; Jansen, M. *Chem. Ber.* **1996**, *129*, 773−777. (c) Seyeda, H.; Armbruster, K.; Jansen, M. *Chem. Ber.* **1996**, *129*, 997−1001. (d) Klein, W.; Armbruster, K.; Jansen, M. *Chem. Commun.* **1998**, *6*, 707−708. (e) Klein, W.; Jansen, M. *Z. Naturforsch.* **1999**, *54b*, 1345−1349.
(43) Dietzel, P. D. C.; Jansen, M. *Chem. Commun.* **2001**, 2008−2009.
(44) Stalke, D. *Chem. Soc. Rev.* **1998**, *27*, 171−178.
(45) Sheldrick, G. M. *SHELXS97 and SHELXL97 − Program suite for the solution and refinement of crystal structures*; University of Göttingen, Germany, 1997.

Table 1. Summary of Crystallographic Data for $[N(CH_3)_3(C_6H_5)](O_2)$ (**1**) and $[N(C_4H_9)_4](O_2)\cdot 2.5NH_3$ (**2a**)

	1	**2a**
formula	$C_9H_{14}NO_2$	$C_{16}H_{43.5}N_{3.5}O_2$
formula weight, g mol^{-1}	168.21	317.04
T, K	123(1)	93(2)
crystal system	orthorhombic	monoclinic
space group	$P2_12_12_1$	$C2/c$
Z	4	8
a, Å	7.0496(11)	23.560(5)
b, Å	9.9887(14)	13.386(3)
c, Å	12.550(2)	15.539(3)
β	90°	124.76(3)°
V, Å^3	883.8(2)	4026.0(14)
λ, Å	0.71073 (Mo Kα)	0.56085 (Ag Kα)
ρ_{calcd}, g cm^{-3}	1.264	1.046
μ, mm^{-1}	0.089	0.044
crystal size, mm	0.2 × 0.1 × 0.05	0.6 × 0.6 × 0.4
F(000)	364	1440
2θ range	3.24−60°	4.44−47°
hkl collected	$-9 \le h \le 9$, $-14 \le k \le 14$, $-17 \le l \le 17$	$-33 \le h \le 33$, $-19 \le k \le 19$, $-21 \le l \le 21$
no. reflections measured	3022	40 651
no. unique reflections	1492 (R_{int} = 0.0429)	6001 (R_{int} = 0.0888)
no. observed reflections	1210	4590
no. reflections used in refinement	1492	6001
no. parameters/restraints	152/46	363/14
R indices ($I > 2\sigma$)[a]	R_1 = 0.0439	R_1 = 0.0576
	wR_2 = 0.1057	wR_2 = 0.1293
R indices (all data)	R_1 = 0.1178	R_1 = 0.0633
	wR_2 = 0.1178	wR_2 = 0.1413
GOF	1.051	1.045
final difference peaks, e/Å^3	+0.248, −0.313	+0.716, −0.373

[a] $R_1 = \sum||F_o| - |F_c||/\sum|F_o|$; w$R_2 = \{\sum[w(F_o^2 - F_c^2)^2]/\sum[w(F_o^2)^2]\}^{1/2}$.

Ne laser (λ = 632.8 nm). The samples were sealed in capillaries of ∅1 mm under dry argon and kept at −78 °C until time of measurement.

Thermal investigations were performed in argon atmosphere using a Netzsch STA 429 DTA-TG measurement device.

The EPR spectra were measured with a Bruker ER040XK microwave X-band bridge and a Bruker BE25 magnet equipped with a BH15 field controller calibrated against DPPH. Samples were sealed in Suprasil quartz glass ampules and cooled in an Oxford Instruments ESR 910 continuous flow He cryostat. The spectra were fitted with the Powfit program in the NIEHS public EPR software package refining the diagonal g tensor components g_x, g_y, and g_z and parallel and perpendicular line widths.[50]

Magnetic susceptibilities were determined with a MPMS7 Quantum Design SQUID magnetometer at magnetic fields of 0.1, 1, 3, and 5 T in the temperature range of 2−240 K. Powder samples were sealed into Suprasil quartz glass tubes filled with helium gas enabling rapid thermal equilibration. The data were corrected for the magnetizations of the individual empty sample holders. Temperature-independent contributions (χ_0) to the magnetic susceptibility were calculated from the high-temperature range using a modified Curie−Weiss law $\chi_{exp} = C/(T - \Theta) + \chi_0$. χ_0 amounted to 2.4(1) × 10^{-4} and 1.8(2) × 10^{-4} emu/mol for **1** and **2b**, respectively. The data were analyzed by fitting them to the Curie−Weiss law in the complete temperature range for the measurement at 0.1 and 1 T and from 75 to 240 K for all measurements because of saturation effects at higher field strengths. The values of the effective magnetic moments and Weiss parameters were then averaged. The weighing error was included in calculating the standard deviations of the effective magnetic moments of **1** and **2**.

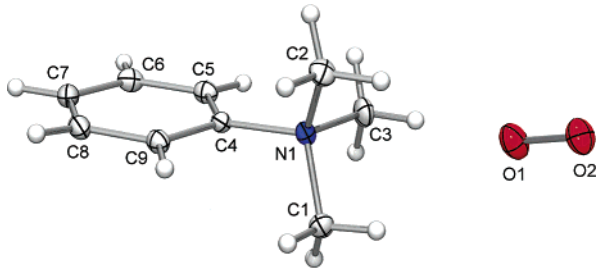

Figure 1. X-ray molecular structure of **1** with atom labeling scheme and ellipsoids drawn at the 50% probability level.

Results

Crystal Structure of $[N(CH_3)_3(C_6H_5)](O_2)$ (1). The crystal structure contains one trimethylphenylammonium ion and one superoxide ion in the asymmetric unit as shown in Figure 1. The bond length of the superoxide ion was determined to 1.332(2) Å. The closest intermolecular distance between neighboring superoxide ions is larger than 5 Å. Distances and angles in the cation are as expected, and they are included in the Supporting Information.

There are nine close contacts in the range from 3.20 to 3.40 Å between the superoxide ion and carbon atoms. These carbon atoms bond to hydrogen atoms that point toward the superoxide ion. Such a geometric arrangement is generally accepted to indicate a possible weak C−H···O bond, especially if the carbon atom in question is located in the α-position to an ammonium group.[46,47] However, in the present case, the contacts of the anion with the trimethylammonium group rather resemble the coordination found for a halide anion that tries to approach the cationic charge. This inevitably leads to close contacts with the methyl groups that inhibit further approach to the center of the cationic charge distribution, which coincides with the nitrogen atom.[47] The close contacts belong to a total of six cation molecules. The centers of gravity of the cations, which are approximately at the positions of C4, form a distorted octahedron. The octahedra are linked via common faces to chains. Adjacent chains are connected by shared edges. This arrangement resembles that in the nickel arsenide structure type. However, because of the aspherical shape of the ions, the superoxide ion is displaced from the center of the coordination polyhedron. The packing and derivation of the crystal structure of **1** from the NiAs-type are shown in Figure 2.

Due to the large distances between the cationic and anionic charge centers and between nearest neighbor superoxide ions, we expect that the electronic properties of the superoxide anion in **1** are largely uninfluenced by its surroundings.

Crystal Structure of $[N(C_4H_9)_4](O_2)\cdot 2.5NH_3$ (2a). The asymmetric unit of **2a** is shown in Figure 3 and contains one cation and anion each and three ammonia molecules, of which one is located in a special position. The bond length of the superoxide amounts to 1.312(2) Å. Bond lengths and angles of

(46) (a) Taylor, R.; Kennard, O. *J. Am. Chem. Soc.* **1982**, *104*, 5063−5070. (b) Taylor, R.; Kennard, O. *Acc. Chem. Res.* **1984**, *17*, 320−326. (c) Desiraju, G. R. *Acc. Chem. Res.* **1991**, *24*, 290−296. (d) Harmon, K. M.; Santis, N. J. D.; Brandt, D. O. *J. Mol. Struct.* **1992**, *265*, 47−57. (e) Desiraju, G. R. *Acc. Chem. Res.* **1996**, *29*, 441−449. (f) Steiner, T. *Cryst. Rev.* **1996**, *6*, 1−57. (g) Steiner, T. *Angew. Chem.* **2002**, *114*, 50−80. (h) Desiraju, G. R. *Acc. Chem. Res.* **2002**, *35*, 565−573.
(47) Desiraju, G. R.; Steiner, T. *The Weak Hydrogen Bond*; Oxford University Press: New York, 1999.
(48) Holzer, W.; Murphy, W. F.; Bernstein, H. J.; Rolfe, J. *J. Mol. Spectrosc.* **1968**, *26*, 543−545.
(49) Fee, J. A.; Valentine, J. S. In *Superoxide and Superoxide Dismutases*; Michelson, A. M., McCord, J. M., Fridovich, I., Eds.; Academic Press: New York, 1977.
(50) Lazos, G. P.; Hoffmann, B. M.; Franz, C. G. *POWFIT Programm for Fitting and Simulating Anisotropic ESR-Spectra, QCPE program number 265, Quantum Chemistry Program Exchange*; Indiana University, Bloomington, Indiana.

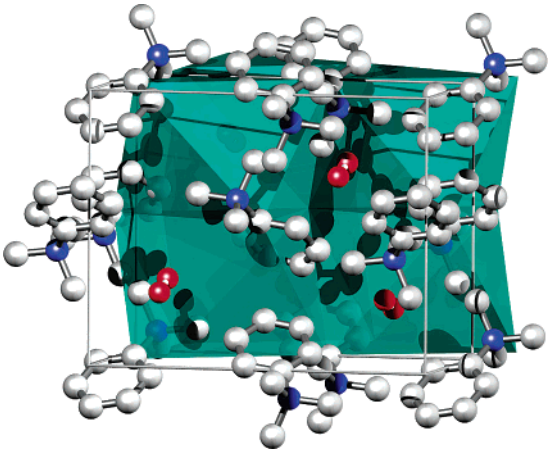

Figure 2. Crystal structure of **1** with coordination polyhedra illustrating the analogy to the nickel arsenide structure type.

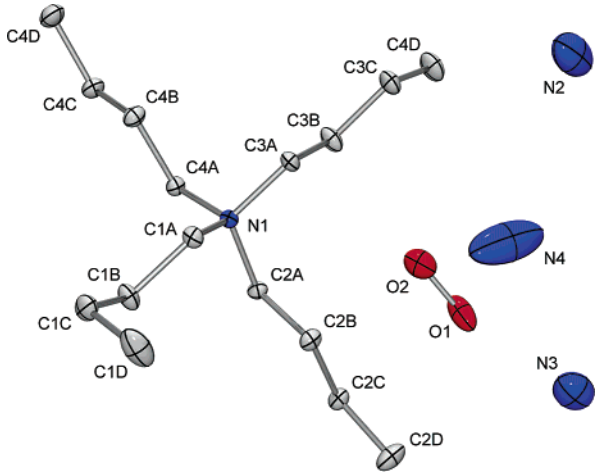

Figure 3. X-ray molecular structure of **2a** with atom labeling scheme and ellipsoids drawn at the 50% probability level.

the cation are in the range of expected values. The tetrabutylammonium cation and superoxide anion in **2a** are well located in the crystal structure. However, the magnitude of the thermal displacement ellipsoids of the nitrogen atoms of the ammonia molecules is much larger than that of the atoms which are part of the cation and anion. In the crystal structure, the ammonia molecules occupy positions in channels parallel to the *c* axis (Figure 4). It is likely that the ammonia molecules have a certain degree of freedom of movement in these channels during crystallization and that this causes the disorder observed in the form of the large thermal displacement parameters found in the structure refinement. The intermolecular distances indicate that the ammonia molecules form hydrogen bonds among each other as well as to the superoxide ion.

Thermal Stability of $[N(CH_3)_3(C_6H_5)](O_2)$ (1). While the superoxides of the heavier alkali metals potassium, rubidium, and cesium are thermodynamically stable, tetraorganylammonium superoxides are metastable compounds that decompose exothermically upon heating. In DTA-TG measurements of **1**, decomposition occurred rapidly above 50 °C. At room temperature, decomposition occurs more slowly. Samples stored in a capillary under argon appear visually unchanged for about a day, but soon thereafter decompose to a yellow liquid containing gas bubbles.

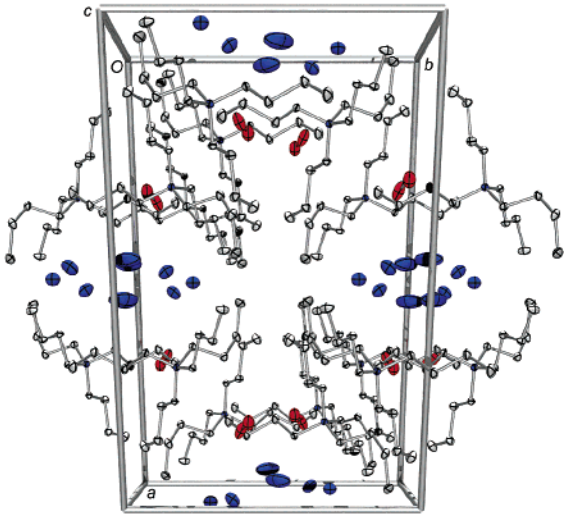

Figure 4. Packing of **2a** along [001] showing the channels occupied by the solvent molecules.

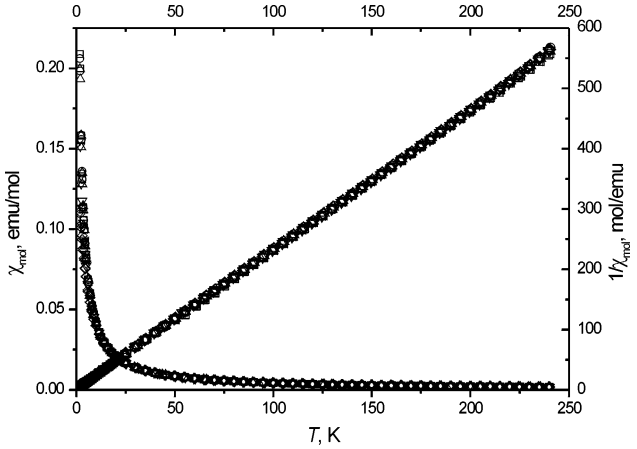

Figure 5. Temperature dependence of the magnetic susceptibility and its inverse of **1** measured at magnetic fields of 0.1, 1, 3, and 5 T.

Vibrational Spectroscopy. Raman spectroscopy of **1** shows the symmetric stretching mode of the superoxide ion at 1121 cm^{-1} and the first overtone at 2224 cm^{-1}, which is in good accord with the wavenumber of 1123 cm^{-1} previously reported for tetramethylammonium superoxide.[40] The superoxide symmetric stretching mode of **2b** is found at 1131 cm^{-1}.

Magnetic Susceptibility Measurements. The molar magnetic susceptibilities $\chi_{mol} = \chi_{exp} - \chi_0$ of **1** are plotted in Figure 5. The corresponding figure for **2b** is virtually identical and is contained in the Supporting Information. The data for all magnetic fields agree very well within error bars. For both compounds, the χ_{mol}^{-1} versus T plots reveal straight lines that intersect the origin, which proves that the compounds do not pass through any magnetic phase transitions above 2 K. The data for the different magnetic fields were fitted to a Curie Weiss law $\chi_{mol} = C/(T - \theta)$ and averaged to yield effective magnetic moments of 1.86(2) μ_B for both compounds. These moments significantly exceed the spin-only value of 1.73 μ_B expected for a single spin radical. The Weiss parameters θ amount to 0.0(4) K for **1** and −0.4(4) K for **2b**, which indicates that there is no detectable exchange interaction between the superoxide ions in both compounds.

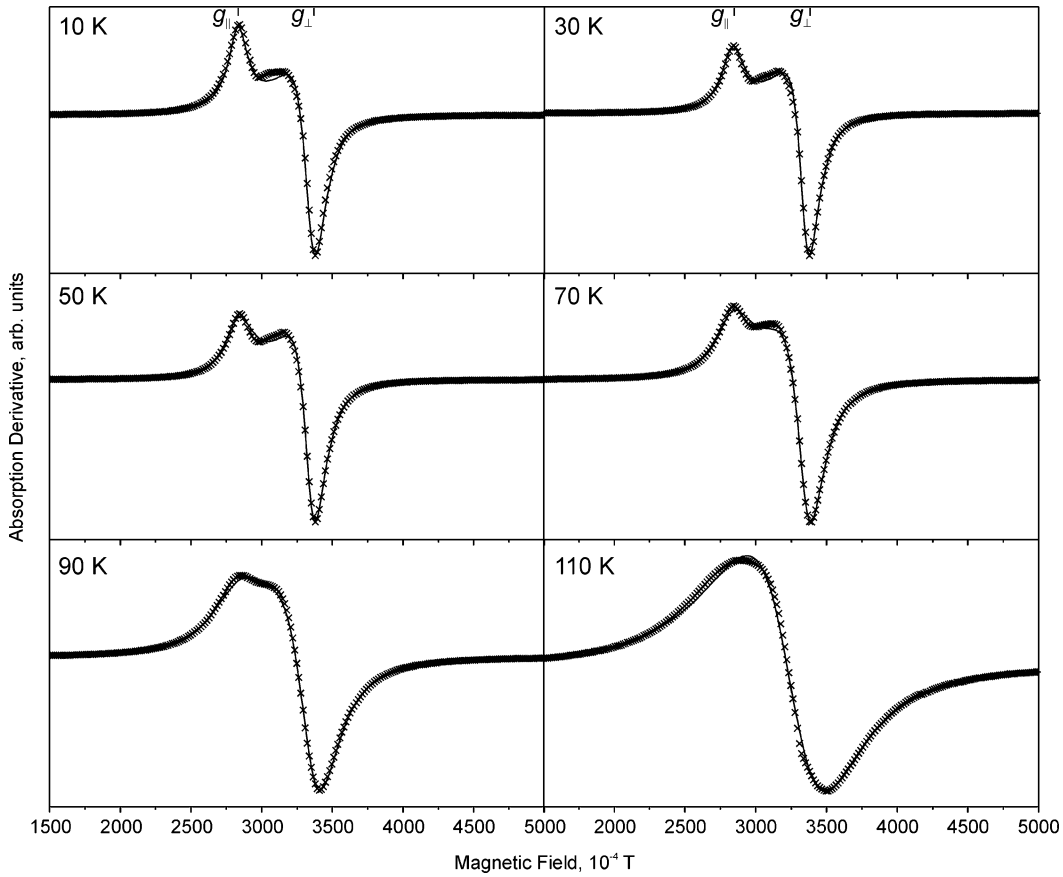

Figure 6. Experimental values and fits (solid line) of the EPR spectra of **1** at the indicated temperatures.

Electron Paramagnetic Resonance Measurements. The EPR measurements of **1** and **2b** show typical powder spectra with a considerable anisotropy of the *g* factors. The signal intensities decrease proportional to $1/T$ from 10 K to approximately 75 K. At higher temperatures, the signal intensities are so weak that the integration becomes increasingly unreliable, and the intensities start to deviate accordingly from the Curie law. Toward higher temperatures, the spectral line widths increase, and above 100 K the spectra become almost symmetric in shape. This behavior is in accordance with the observations made on frozen solutions containing the superoxide ion[49] and on single crystals of KO_2.[30] The diagonal elements of the *g* tensors of **1** and **2b** are obtained by fitting the spectra (Figures 6 and 7) and are listed in Table 2. For **1**, the *g* tensor is to a high degree axially symmetric with $g_x \cong g_y$, while for **2**, the three components of the *g* tensor have significantly different values each. The average g_{av} values derived from $g_{av} = {}^1/_3(g_x + g_y + g_z)$ are in accordance with each other. Due to the increasing line widths, the determinations of the *g* values from the spectra above 100 K are fairly imprecise, and only the values from 10 to 90 K have been used for averaging.

Discussion

Two cases, one pertaining to the bond length of the superoxide and the other to its magnetic properties, have to be differentiated when analyzing the experimental results with respect to whether they are representative of the properties of a superoxide ion that is as unperturbed as possible in the solid state. The bond length in the superoxide ion is dependent on the entire environment of the superoxide ion. Both Coulombic interactions with the surrounding ions and hydrogen bonding affect the electron density in the superoxide ion. Therefore, the former have to be minimized, and the latter should be absent to obtain a precise value of an O−O distance that can be taken as characteristic for the virtually isolated superoxide ion. The frequency of the O−O stretching mode allows for an estimate of the strength of the interaction between the superoxide ion and its vicinity. In addition, the superoxide ion needs to be locked as precisely as possible in its position to yield a reliable bond length in the structure determination. In **1** and **2a**, the aspherical shape of the cations allows for an optimal packing arrangement that does not permit the superoxide ion to perform significant motion nor crystallize in strongly disordered positions. In contrast to the bonding properties of the superoxide ion, the magnetic properties are only influenced by exchange interaction via the radical anions themselves. In compounds **1** and **2b**, the magnetic susceptibility adheres to the Curie law ($\theta = 0$), which indicates the unprecedented absence of sizable exchange interactions between the superoxide ions. The observed magnetic moments, which are larger than the expected spin-only value for a single spin system, are in agreement with the average *g* factors obtained from the EPR measurements. Their deviation from the spin-only value can be understood from the electronic structure of the superoxide ion in the solid state.

The Electronic Structure of the Superoxide Ion. The superoxide ion has the electron configuration $1\sigma_g^2 1\sigma_u^{*2} 2\sigma_g^2 2\sigma_u^{*2} 3\sigma_g^2 1\pi_u^4 1\pi_g^3 3\sigma_u^0$. The two π_g orbitals are composed of the p_x and p_y oxygen atomic orbitals. In molecular oxygen, the π_g orbitals are degenerate and each orbital is occupied by one electron. In the superoxide ion, another electron is added, so

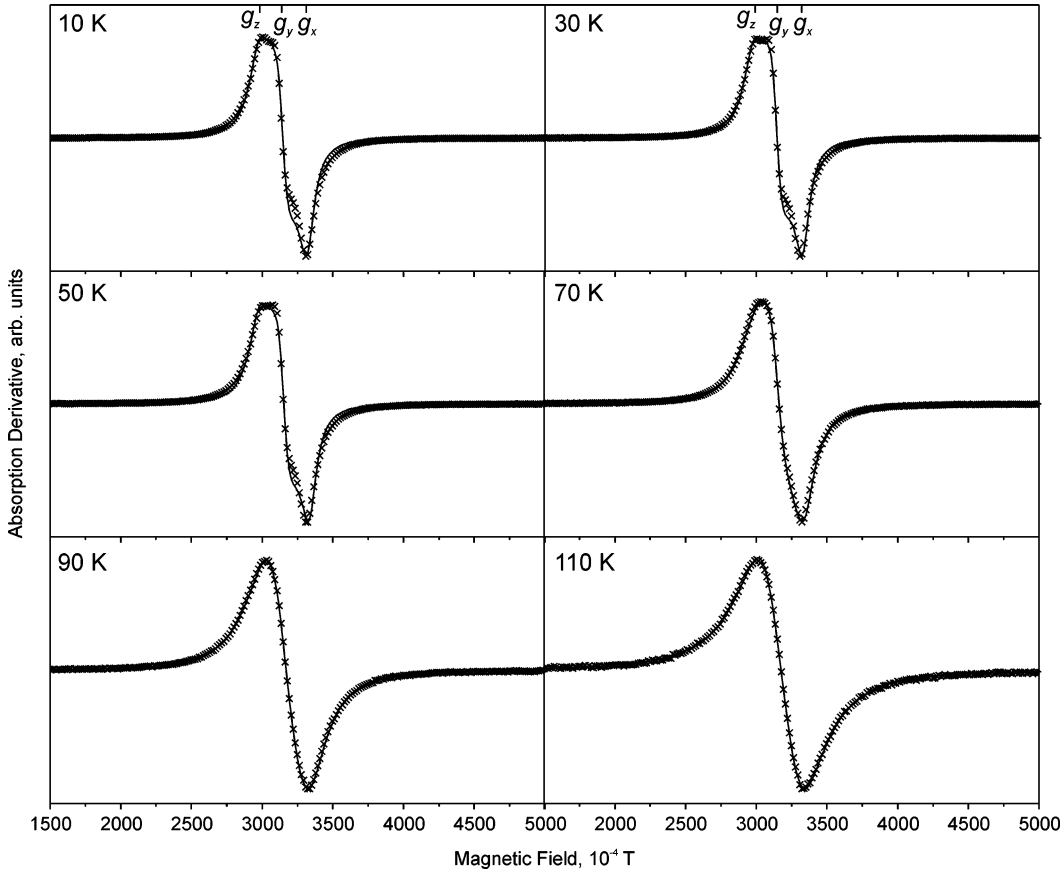

Figure 7. Experimental values and fits (solid lines) of the EPR spectra of **2b** at the indicated temperatures.

Table 2. Values of the Diagonal Elements of the *g* Tensors of **1** and **2b** Obtained from Fitting the Spectra at Different Temperatures

cmpd	*T*, K	g_x	g_y	g_z	g_{av}
1	10	1.984	1.983	2.339	2.102
	30	1.984	1.983	2.337	2.101
	50	1.985	1.985	2.337	2.102
	70	1.986	1.984	2.337	2.102
	90	1.986	1.986	2.336	2.103
	110	2.015	2.014	2.236	2.088
	10−90	1.985	1.984	2.337	2.102
2b	10	2.000	2.112	2.230	2.114
	30	1.990	2.108	2.225	2.108
	50	1.987	2.103	2.225	2.105
	70	1.987	2.108	2.221	2.105
	90	1.996	2.117	2.183	2.099
	110	2.018	2.149	2.131	2.099
	10−90	1.992	2.110	2.217	2.106

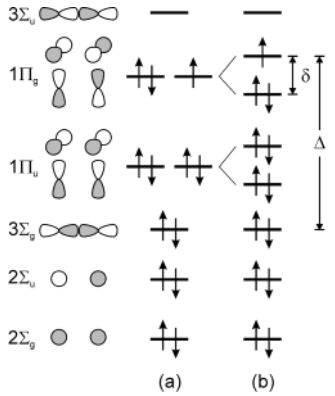

Figure 8. Schematic drawing (not to scale) of the valence electron energy levels in the free superoxide ion in the gas phase (a) and in the crystal field of a solid of lower than cubic symmetry (b).

that one π_g orbital is fully occupied and the other one contains a single electron. While both levels remain degenerate in the gas phase (Figure 8a), the unequal occupation allows for several possible consequences in the solid state: If the crystal field experienced by the superoxide ion is of orthorhombic symmetry, it will interact differently with each of the molecular orbitals. As a result, the degeneracy of the energy levels will be removed, and the lower lying energy level will be occupied by two electrons, while the remaining electron will inhabit the HOMO (Figure 8b). In this case, the magnetic moment will exhibit the spin-only value. On the other hand, if the orbital momentum is not quenched, the spin−orbit coupling will result in a magnetic moment of 2 μ_B.[22] In fact, the degeneracy of the Π_g^x and Π_g^y energy levels is removed in the solid state, but some contribution of the orbital momentum to the magnetic moment remains.[52] The energy splitting δ between the nondegenerate Π_g levels and the overall splitting Δ between the Σ_g and the upper Π_g levels determine the deviation of the *g* factor from the free electron value. Theoretical derivations of the electronic structure of the superoxide ion in static crystal fields of orthorhombic and monoclinic symmetry have yielded accurate expressions for these deviations,[52,54−57] which can be simplified into the

(51) Travers, M. J.; Cowles, D. C.; Ellison, G. B. *Chem. Phys. Lett.* **1989**, *164*, 449−455.
(52) Baumann, R.; Beyeler, H. U.; Känzig, W. *Helv. Phys. Acta* **1971**, *44*, 252−278.
(53) Johnston, R. S.; Osgood, E. D.; Miller, R. R. *Anal. Chem.* **1958**, *30*, 511−513.

easily applicable forms:[56,58]

$$\Delta g_x = 2(\lambda/\Delta) - (\lambda^2/\delta^2) \quad (1)$$

$$\Delta g_y = -(\lambda^2/\delta^2) \quad (2)$$

$$\Delta g_z = 2(\lambda/\delta) \quad (3)$$

λ is the spin−orbit coupling constant for the superoxide ion, for which values in the range of 113−226 cm^{-1} have been suggested in the literature.[32,54−56,58]

Raman Spectroscopy. The symmetric stretching vibration of the superoxide ion in **1** and **2b** indicates that the superoxide ions in both compounds experience only a low level of intermolecular interaction. With values of 1121 and 1131 cm^{-1} for **1** and **2b**, respectively, the energies of the stretching vibration in the tetraorganylammonium superoxides **1** and **2b** fit into the trend observed for the alkali metal superoxides, for which the energies of the stretching mode decrease with increasing cation size from 1164 cm^{-1} for NaO_2 to 1136 cm^{-1} for CsO_2.[23] Concurrently, the polarizing strength of the cation decreases. The value for the free O_2^- species has been calculated to be 1090 cm^{-1},[48] and this value is approached by the frequency of the stretching mode in **1** and **2b**. Both compounds show no vibrations of ammonia in the Raman spectra. For **1**, this is expected from the crystal structure. In the case of **2b**, it shows that the removal of the ammonia from the structure is complete.

Crystal Structures. The alkali metal superoxides undergo several structural phase transitions that hamper a reliable determination of the O−O distance, and the results of the structure determinations of the alkali metal superoxides[4,7,9−11,15,18,21,27,28] are not in agreement with each other and lack precision. [The high-temperature phase of each of the alkali metal superoxides MO_2 (M = Na, K, Rb, Cs) derives from the NaCl structure type,[7,9,10,21,27] in which the orientation of the superoxide ion has been addressed as disordered,[7] freely rotating,[9] or performing a hindered rotation.[10] For this phase of NaO_2, bond lengths of 1.31(3), 1.33(6), and 1.37(1) Å have been reported for the superoxide ion.[7,9,27] At lower temperatures, NaO_2 crystallizes in the pyrite structure type, for which a O−O bond length of 1.35(5) Å has been published,[27] and in the marcasite structure type, for which O−O bond lengths of 1.28(10) and 1.31 Å have been found.[10,27] The O−O distance has been experimentally determined for the room-temperature phase of KO_2, which crystallizes in the CaC_2 structure type. The obtained values of 1.28(7) and 1.28(2) Å are possibly underestimated because of the large thermal displacement parameters.[4,11] The same diffraction data agree with a bond length in the range of 1.32−1.35 Å,[15] if the superoxide ion performs a precession around the tetragonal axis. This motion would also account for the large temperature factors in the above-mentioned experimental reports. When the axis of the superoxide ion was tilted with respect to the tetragonal axis, the anion occupies an energetically more favorable position. Therefore, the range of 1.32−1.35 Å represents probably the best estimate of the bond length in the superoxide ion available until now. The bond length of 1.19 Å in the room-temperature phase of CsO_2,[27] which is isostructural to the room-temperature phase of KO_2, deviates strongly from all of the other reported values for the O−O distance.] The only additional determination of the O−O distance in the superoxide ion has been carried out on 1,3-bis(trimethylammonium)benzene disuperoxide ammoniate.[41] This compound contains ammonia that forms hydrogen bonds with the superoxide ions, which are expected to influence the electronic structure and therefore the bond length of the superoxide ion. This also is the case for **2a**, in which the O−O distance is slightly shorter than that in **1**. The hydrogen bonding between the superoxide ion and the ammonia molecules leads to a polarization of the electron density distribution in the superoxide ion. With respect to a superoxide ion that is not subjected to hydrogen bonding, there will be some redistribution of electron density toward the hydrogen atom. This will affect most the least tightly bound electrons in the superoxide ion. These are the electrons in the antibonding HOMO, and their redistribution may result in a stronger bond in the superoxide ion which is reflected by the shorter bond length.

In contrast, the crystal structure of **1** does not contain any ammonia molecules that may influence the electronic structure of the superoxide ion. Additionally, the trimethylphenylammonium cation is sufficiently large to reduce the Coulombic interactions between these ions, and its aspheric shape results in an adequate localization of the superoxide ion. As a result, the structure determination described in this report represents to date the most reliable determination of the O−O distance in a superoxide ion in the solid state, which to the greatest possible extent is unperturbed by its environment. This interpretation is strongly supported by the fact that a bond length of 1.347(5) Å has been found for the superoxide ion in the gas phase.[51] As the superoxide ion in the gas phase does not experience any strong interactions with its surroundings, the small decrease of the bond length found in **1** with respect to that in the gas phase attests to the weak nature of the crystal field interactions in **1**.

Magnetic Susceptibility. Contrary to the alkali metal superoxides, the superoxide ions in **1** and **2b** are magnetically well isolated. The antiferromagnetic exchange as reflected by the Weiss parameter decreases with increasing size of the cation in the room-temperature phases of the alkali metal superoxides.[22] We therefore ascribe the absence of noticeable exchange interactions in **1** and **2b** to the increased size of the cations with respect to the alkali metal ions.

Identical values of the magnetic moment were obtained for **1** and **2b**. This is expected, if both compounds are representative of the noninteracting superoxide ion. The identity of the magnetic moments also indicates that **2b** contains the paramagnetic superoxide ion in the bulk. In coherence with the result from the Raman spectrum that **2b** does not contain any ammonia, we conclude that **2b** is the pure tetrabutylammonium superoxide compound. In contrast to the results for **1** and **2b**, the alkali metal superoxides have different magnetic moments depending on the metal element and modification under investigation.[5,17,22,40,53] The deviation of the observed effective magnetic moments of **1** and **2b** of 1.86(2) μ_B from the spin-only value of $\sqrt{3}$ μ_B is due to contributions of the orbital momentum. The magnitude of the spin−orbital contribution to the magnetic moment is confirmed by the g factors obtained from the electron paramagnetic resonance spectra of **1** and **2b**.

(54) Känzig, W.; Cohen, M. H. *Phys. Rev. Lett.* **1959**, *3*, 509−510.
(55) Zeller, H. R.; Känzig, W. *Helv. Phys. Acta* **1967**, *40*, 845−872.
(56) Kasai, P. H. *J. Chem. Phys.* **1965**, *43*, 3322−3327.
(57) Shuey, R. T.; Zeller, H. R. *Helv. Phys. Acta* **1967**, *40*, 873−886.
(58) Lindsay, D. M.; Garland, D. A. *J. Phys. Chem.* **1987**, *91*, 6158−6161.

Table 3. Experimental and Calculated Values of the Effective Magnetic Moment and the Average *g* Factor

cmpd	μ(exp), μ_B	μ(calc), μ_B	g_{av}(exp)	g_{av}(calc)
1	1.86(2)	1.82	2.102	2.15(3)
2b	1.86(2)	1.82	2.106	2.15(3)

The average *g* value can be used to calculate the effective magnetic moment via

$$\mu_{\text{eff}} = g\sqrt{S(S+1)} = {}^1/_2 g\sqrt{3}$$

and vice versa. A comparison between the experimental results and the calculated values is given in Table 3.

Electron Paramagnetic Resonance. The diagonal elements of the *g* tensor for **1** and **2** have markedly different values. However, the average values of *g* for **1** and **2b** concur with each other. While the values for **1** reflect the axial symmetry of the superoxide ion, the values for **2b** differ strongly in all three directions. We attribute this to reduced symmetry in the structure of **2b**, which cannot be verified currently, because the crystallinity of **2a** is lost upon removal of the solvent ammonia molecules. In any case, the values of the diagonal elements are within the range found previously for the alkali metal superoxides[12,22,31] and superoxide centers in alkali metal halides.[52,54,55] In both of these systems, the values of the diagonal elements also vary widely depending on the counterion and also the halide ion in the case of the doped alkali metal halides.

Equations 1−3 can be used to estimate the energy splittings of the Π_g molecular orbitals in the superoxide ion for **1**. For the spin−orbit coupling constant λ, we adopt the value of 200 cm^{-1}.[32] For the equations to be applicable, g_x must be $\approx g_y$, which is valid for orthorhombic and monoclinic point symmetry of the superoxide position. This is not the case for **2b**, where the experimental values of g_x and g_y differ too much from each other. In the temperature range from 10 to 90 K, the deviations from the free electron value for **1** are $\Delta g_x = -0.017$, $\Delta g_y = -0.018$, and $\Delta g_z = 0.335$. From these results and eqs 2 and 3, the splittings of the Π_g levels in the crystal field are calculated to be 1491 and 1194 cm^{-1}, respectively. From eq 3, $\Delta g_z/2 = \lambda/\delta$, and eq 1, we obtain $\Delta \approx 39\,000$ cm^{-1}. The error in the value of Δ is much larger (of the order of several thousand cm^{-1}), though, than that of the value of δ, because the quadratic term in eq 1 also amplifies the error of the measured Δg values.

Several EPR studies on a number of systems have yielded values for the energy splitings δ and Δ in the superoxide ion that can be used for comparison. Values of $\delta = 4033$ cm^{-1} and $\Delta = 29\,842$ cm^{-1} have been found for the superoxide ion in zeolites.[56] In matrix isolated alkali metal superoxides, δ is in the range of 2490−2870 cm^{-1} (alkali metal = sodium to cesium) and 5400 cm^{-1} for lithium superoxide, and Δ is in the range of 36 000−44 000 cm^{-1}.[58] For the superoxide ion in alkali metal halides, δ is found to be in the range of 707−1481 cm^{-1}, and Δ is of the order of 40 000 cm^{-1}.[55] Thus, the magnitude of the values in the present report compares well with the literature data. In addition, it is apparent that Δ is largely independent of the type of compound, as is expected for a parameter that is supposed to be an intrinsic property of the superoxide ion, while δ is directly influenced by the environment surrounding the superoxide ion.

Conclusions

By replacing the spherical alkali metal cation by large aspherical tetraorganylammonium ions, we have obtained superoxide compounds with large distances between adjacent superoxide ions and between the cationic and anionic charges. We have found the superoxide ion in **1** and **2b** to be unperturbed by magnetic interactions. As a result, **1** and **2b** are well suited to study the physical properties of the virtually unperturbed superoxide ion in the solid state. The magnetic moments in **1** and **2b** are larger than expected for a spin-only moment. This is ascribed to spin−orbit coupling intrinsic to the superoxide ion. The values of the magnetic moments are confirmed by the *g* factors obtained from electron paramagnetic resonance spectra. The anisotropy of the diagonal elements of the *g* tensor of **1** has been used to estimate the energy gaps in the superoxide ion. The O−O distance in the superoxide ion in the crystal structure of **1** is representative of the largely interaction-free superoxide ion in the solid state, while in **2a** hydrogen bonding to solvent ammonia molecules contained in the structure draws electron density from the superoxide ion and leads to a slightly decreased bond length in the superoxide ion.

Acknowledgment. We thank Sanela Kevrić for assistance with the preparative work, Dr. Oliver Oeckler for collecting the single-crystal X-ray data of **2a**, Eva Brücher for the magnetic susceptibility measurements, and Dr. Hans Vogt for recording the Raman spectrum of **2b**.

Supporting Information Available: Crystallographic data in CIF file format, magnetic susceptibilities of **2b**, figures of fits of the magnetic susceptibilities, and figures of the EPR data of **1** and **2b** in the complete temperature range (PDF). This material is available free of charge via the Internet at http://pubs.acs.org.

JA039880I